

# A 6-bit 3.3GS/s Current-Steering DAC with Stacked Unit Cell Structure

Si-Nai Kim, Wan Kim, Chang-Kyo Lee, and Seung-Tak Ryu

**Abstract**—This paper presents a new DAC design strategy to achieve a wideband dynamic linearity by increasing the bandwidth of the output impedance. In order to reduce the dominant parasitic capacitance of the conventional matrix structure, all the cells associated with a unit current source and its control are stacked in a single column very closely (stacked unit cell structure). To further reduce the parasitic capacitance, the size of the unit current source is considerably reduced at the sacrifice of matching yield. The degraded matching of the current sources is compensated for by a self-calibration. A prototype 6-bit 3.3-GS/s current-steering full binary DAC was fabricated in a 1P9M 90 nm CMOS process. The DAC shows an SFDR of 36.4 dB at 3.3 GS/s Nyquist input signal. The active area of the DAC occupies only 0.0546 mm<sup>2</sup> (0.21 mm x 0.26 mm).

**Index Terms**—DAC, wideband dynamic linearity, stacked unit cell

## I. INTRODUCTION

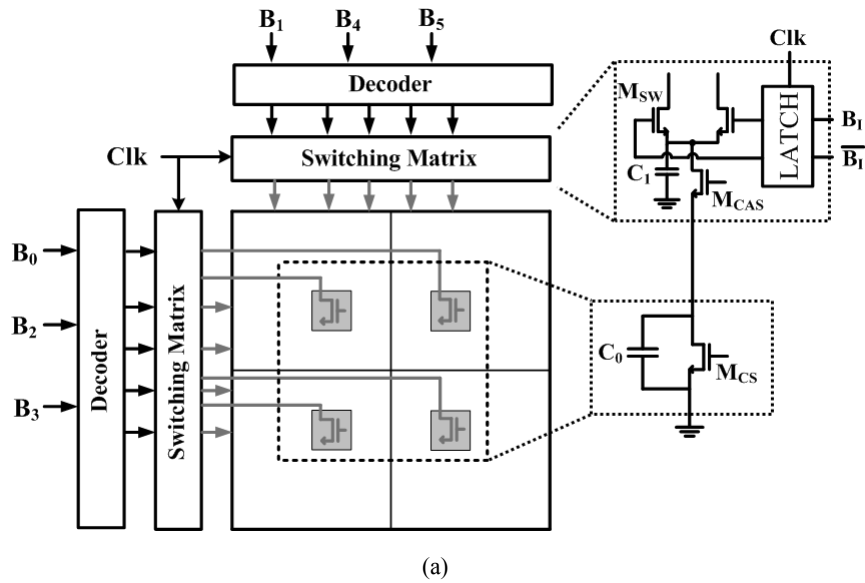
Emerging high speed data communication systems such as 60-GHz WPAN and ultra-wideband (UWB) radios require high speed data converters with GHz-order sampling rates. One of the critical design issues with high speed DACs is how to preserve the dynamic linearity (spurious free dynamic range, SFDR) at high frequency signals while avoiding reduction of the output

impedance [1, 2]. The common-centroid based two-dimensional (2-D) current source array [2, 3] is a suitable DAC architecture for good static linearity (DNL/INL). However, when it comes to the dynamic linearity, i.e. SFDR, the common-centroid based two-dimensional (2-D) current source array may not be the best choice because of the large parasitic capacitance at the output of the current source. This paper focuses on the dynamic linearity of a high speed DAC and presents a new design strategy to achieve wideband linearity from a high-speed 6-bit current-steering DAC. In order to minimize the parasitic capacitance at nodes in the output current path, this study proposes a stacked unit cell structure that minimizes the length of the interconnection wires. In addition, to further reduce the capacitance, the current source size is considerably reduced at the cost of increased mismatch. The degraded matching yield is compensated for by a self-calibration.

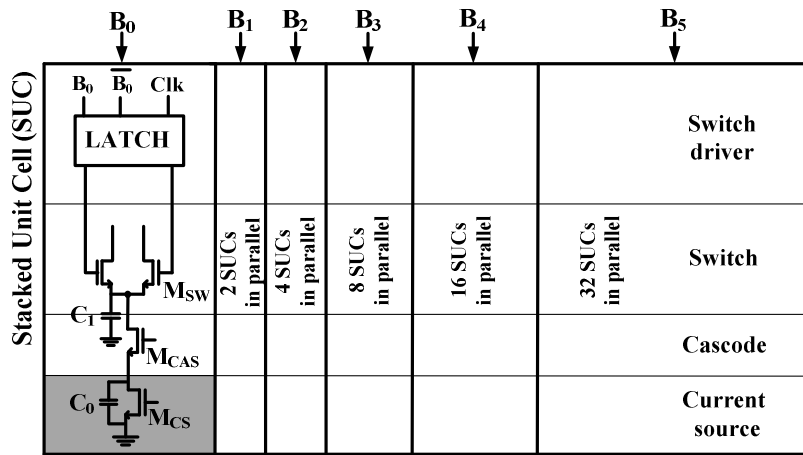
In the next section, design considerations for the wideband DAC are discussed. The proposed wideband DAC architecture is presented in Section III. In Section IV, the self-calibration scheme for the suggested design is explained. Measurement results are discussed in Section V, and Section VI concludes the paper.

## II. DESIGN CONSIDERATIONS FOR WIDEBAND DAC

Fig. 1(a) shows a representative structure of a 2-D current-matrix-based current-steering DAC with a schematic of a 1-bit cell. The structure is good for cell matching owing to the compact current source array, often with common centroid or randomized cell placement [3-5]. However, one drawback with this



(a)



(b)

Fig. 1. (a) Structure of 2D current source array, (b) proposed DAC structure based on SUC.

structure is that the spread of current sources ( $M_{CS}$ ) for better static matching requires relatively long interconnection wires, which results in large parasitic capacitance ( $C_0$ ) at the output of the current sources.

$C_0$  reduces the output impedance as the signal frequency increases and, thus, SFDR degrades. In order to alleviate the effect of  $C_0$  at high frequency, many designs have employed cascode current sources ( $M_{CAS} + M_{CS}$ ) [2, 3] to increase both the static and dynamic output impedance. The cascode transistor ( $M_{CAS}$ ) on top of the current source ( $M_{CS}$ ) provides high output resistance at low frequency. One drawback with the cascode structure might be the added junction capacitance at  $C_0$  by  $M_{CAS}$ .

Even though the cascode current source comes at the expense of increased  $C_0$ , the increased output resistance at DC and small  $C_1$  provides wider bandwidth of output impedance than does the simple current source. Fig. 2 illustrates the output impedance characteristics of the simple current source, the cascode, and the proposed design. Here, it is assumed that the switch transistors ( $M_{SW}$  in Fig. 1) work in the saturation region when they are on. In order to reduce the parasitic capacitance  $C_1$ , the sizes of  $M_{SW}$  and  $M_{CAS}$  can be minimized by considering the operational voltage conditions. Another drawback of the cascode current source that we can think of is that the insertion of  $M_{CAS}$  reduces the available  $V_{DS}$  of  $M_{CS}$ .

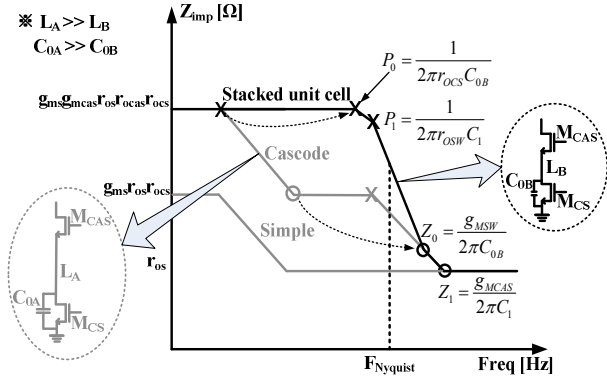


Fig. 2. Frequency response of output impedance.

Therefore, the overdrive voltage ( $V_{OV} = V_{Dsat} = V_{GS} - V_{TH}$ ) of  $M_{CS}$  should be reduced with increased transistor size, which increases  $C_0$ . However, since the routing parasitic at the drain of  $M_{CS}$  is more dominant,  $M_{CS}$  does not increase  $C_0$  substantially in the 2-D structure. A side effect of the reduced  $V_{OV}$  in  $M_{CS}$  is that the current matching characteristic degrades according to (1) [6]. This problem will be revisited in Section III with

$$WL = \left[ A_\beta^2 + \frac{4A_{VT}^2}{(V_{GS} - V_{TH})^2} \right] \frac{I^2}{2\sigma^2(I)} \quad (1)$$

the proposed design.

Even though  $C_0$  has not been a serious problem, as the sampling frequency further increases to more than several GHz, it can be difficult to secure sufficient output impedance up to the Nyquist frequency. As the graph ‘Cascode’ in Fig. 2 illustrates, the long routing line ( $L_A$ ) at the drain node of  $M_{CS}$  makes large capacitance ( $C_{0A}$ ). Thus, if the routing ( $L_B$ ) wire can be shortened the value of capacitance ( $C_{0B}$ ) can be reduced substantially ( $P_0$  can be located close to  $P_1$ ) and consequently the impedance bandwidth will be extended.

### III. PROPOSED WIDEBAND DAC ARCHITECTURE

To extend the bandwidth of the output impedance, the present work focuses on reducing  $C_0$ . Reduction of  $C_0$  is achieved in this work by two design approaches: 1) minimization of the interconnection path from the current source to the current switch, and 2) reduction of the current source size at the expense of degraded matching yield. In order to minimize  $C_0$  from the interconnection

Table 1. Current source size reduction

	$3\sigma$ INL	$V_{ov}$ [V]	WL [ $\mu\text{m}^2$ ]	$(W/L)_{CS}$ [ $\mu\text{m}^2$ ]	$C_0$ [fF]	Comparison (WL)
(a)	6-bit	0.11	3.68	8.3/0.4	10.1	1
(b)	4-bit	0.15	0.51	2.3/0.2	3.1	0.14

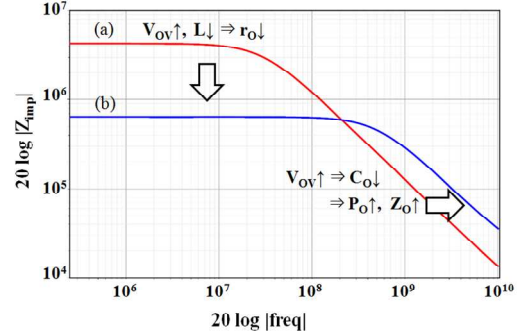


Fig. 3. Bandwidth variation according to  $V_{OV}$  and INL yield.

lines, all the elements for a unit current cell, including its control, are stacked in a single column; the structure is referred to as a Stacked Unit Cell (SUC) in this paper, as the  $B_0$  cell in Fig. 1(b) illustrates. In order to avoid design complexity, the DAC was designed in a full binary-weighted manner. Since  $M_{CS}$ ,  $M_{CAS}$ ,  $M_{SW}$ , and a latch for switch driving are stacked closely, the parasitic capacitances due to the interconnection lines between them, i.e.  $C_0$  and  $C_1$ , are minimized. To construct a binary weighted current-steering DAC, all the SUCs are placed in a single line and grouped for binary-weight generation.

This structure provides a very compact layout. In contrast to the traditional 2-D current source array, in which the contribution of the junction capacitance of  $M_{CS}$  is not significant due to the excessive interconnection parasitic capacitance, the proposed SUC structured single-line layout scheme can be dominantly affected by the junction capacitance of the transistors. This implies that the pole frequency  $P_0$  can be pushed to a higher frequency by using a smaller transistor size. Table 1 shows how we were able to reduce  $C_0$  in this design. Since this work targets 6-bit resolution, the required output impedance values  $Z_{imp}$  for 0.5 LSB INL and for 38 dB SFDR are 98.5 K $\Omega$  and 50 K $\Omega$ , respectively [7, 8]. Row (a) in Table 1 is the current source design result for a 6-bit DAC with  $3\sigma$  yield for 0.5LSB INL. In order to further extend the bandwidth of the output impedance, the overdrive voltage of  $M_{CS}$  was increased by 40mV with reduced W/L in order to reduce the current source size (row (b) in Table 1). In addition, we guarantee only a

4-bit linearity (0.5 LSB INL with 3-sigma yield) even though the design target is 6-bit resolution. As row (b) illustrates, the 4-bit matching design with enhanced  $V_{ov}$  and the reduced transistor size reduces the parasitic capacitance by about 1/3 while at which bandwidth of the output impedance (frequency where  $Z_{imp}=50\text{ K}\Omega$ ) is extended 2.5-fold (up to 6 GHz) compared with that of the 6-bit yield design shown in (a).

While the proposed design extends the bandwidth of the output impedance, the DC resistance is degraded due to the reduced output resistance ( $r_o$ ) of the current source, as delineated in (2). However, the output resistance of the unit current source is set at  $650\text{ K}\Omega$ , guaranteeing the required static linearity.

$$I_D = \frac{\mu_n C_{ox} W}{2 L} V_{OV}^2, \lambda \propto \frac{1}{L} \Rightarrow r_o \propto \frac{L^2}{W * V_{OV}^2} \quad (2)$$

In order to minimize glitches during the transition period, the latch introduced in [2] was used. The latch synchronizes the control signals in front of the switch transistors. In addition, by raising the crossing point of the differential input signals, the NMOS switches are not turned off simultaneously and the voltage fluctuation at the source coupled node is mitigated. In order to obtain high frequency input data and clock signal, a typical differential receiver was used [1].

#### IV. SELF-CALIBRATION FOR CURRENT MISMATCH

The degraded matching between the current sources due to the reduced yield design for wideband dynamic linearity in the single line SUC array is compensated for by a self-calibration. Since only a 4-bit linearity is guaranteed by the designed transistor size, current sources for the fifth and sixth bits ( $B_4$  and  $B_5$ ) are calibrated. Fig. 4(a) and (b) illustrate the operational principle of the current source calibration with simple block diagrams, which is a quite popular method [9]. In order to calibrate the  $B_4$  segment (Fig. 4(a)), the currents from the lower bits ( $B_3 \sim B_0$ ) and the dummy current whose amount is the same as that of  $B_0$  are added together and then the added current is compared with the current from the  $B_4$  segment. Until the polarity of the comparator changes, the input code of CAL-DAC is

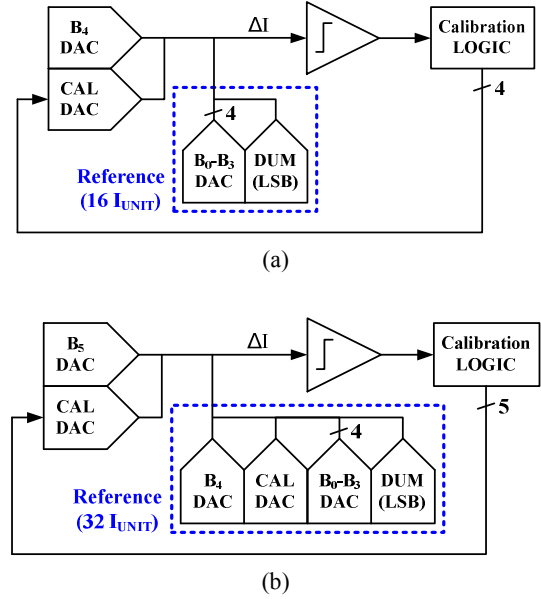


Fig. 4. Block diagram of the self-calibration (a)  $B_4$  DAC (b)  $B_5$  DAC.

controlled. A detailed calibration scheme for  $B_4$  is illustrated in Fig. 5 with a transistor-level circuit diagram.

The main current source array for  $B_4$  (MSB-1 bit) was designed with 15 unit current sources, instead of 16, for a nominal current of  $15 I_{UNIT}$ . The calibration DAC for the  $B_4$  segment (Cal-DAC4) has a 4-bit resolution with LSB current of  $1/8 I_{UNIT}$  and a full current of  $2 I_{UNIT}$ . In its calibration period ( $VC=1$ ), the total current from the termination current source (DUM with  $I_{UNIT}$ ) and  $B_3 \sim B_0$  segments, whose nominal value is  $16 I_{UNIT}$ , is compared with the sum of the current from the  $B_4$  segment and from Cal-DAC4. Cal-DAC4 increases its current until the polarity of the current comparator changes.

The calibration operation for  $B_5$  is similar to that for  $B_4$  except that it operates when  $VC=0$  ( $VCB=1$ ); the calibration DAC for  $B_5$  (Cal-DAC5) has a 5-bit resolution. The  $B_5$  segment has a nominal current of  $30 I_{UNIT}$  instead of  $32 I_{UNIT}$  and Cal-DAC5 has a full current of  $4 I_{UNIT}$ . Since the current comparison is done in the foreground with a different current path, not to the output load, the comparator can incorporate large transistors for small offset. Our Monte-Carlo simulation estimated the 1-sigma offset value of the current comparator at  $2.3\ \mu\text{A}$ , which is sufficiently small for 6-bit DAC calibration because the 1LSB current of the main DAC is  $64\ \mu\text{A}$ . The PMOS load of the comparator was laid out in a common-centroid fashion for offset reduction.

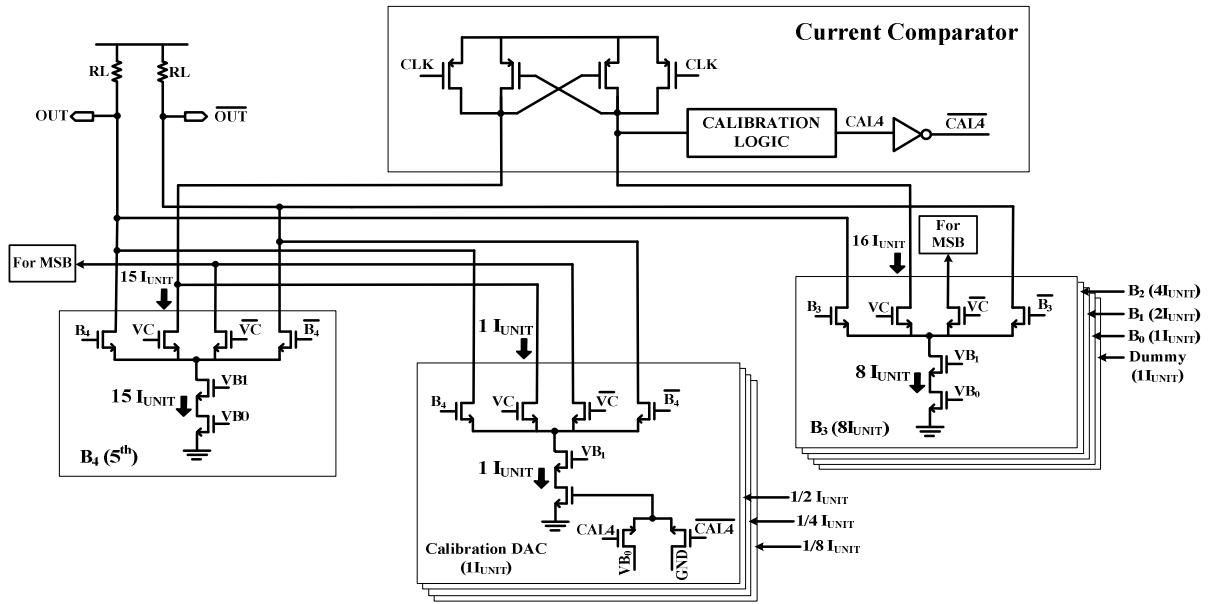


Fig. 5. Calibration scheme for MSB-1( $B_4$ ) bit segment calibration.

V. MEASUREMENT RESULTS

A prototype of the proposed 6-bit DAC was implemented in 90 nm CMOS technology. The chip photo is shown in Fig. 6. Note that the area occupied by the cascode current sources and the switches is as small as  $10 \mu\text{m} \times 260 \mu\text{m}$  owing to the single-line layout. Most of the area of SUC is occupied by the  $100 \mu\text{m}$ -high latches for the switch driver. The total active area, including the loosely drawn calibration control logic, is  $210 \mu\text{m} \times 260 \mu\text{m}$ .

The measured static linearity is shown in Fig. 7. Before calibration, the peak DNL and INL are  $-1 \text{ LSB}$  and  $-0.71 \text{ LSB}$ , respectively. After calibration, the peak DNL and INL are reduced to  $-0.22 \text{ LSB}$  and  $0.25 \text{ LSB}$ .

Dynamic performance was measured at several sampling frequencies. Fig. 8 shows the measured  $46.2 \text{ dB}$  SFDR for  $51 \text{ MHz}$  input signal frequency, at  $3.3 \text{ GS/s}$ .

The SFDR for the Nyquist input at  $3.3 \text{ GS/s}$  is  $36.4 \text{ dB}$  as shown in Fig. 9. Due to the degraded matching property of the signal path on the test board, THD performance is not so good.

The summary of the measured SFDR as a function of signal frequency at  $1 \text{ GS/s}$ ,  $2 \text{ GS/s}$ , and  $3.3 \text{ GS/s}$  is presented in Fig. 10. SFDR at  $3.3 \text{ GS/s}$  ( $0.1 \sim 0.4 \text{ Fsig/Fclk}$ ) is degraded. In the measurement, S11 of the output network on the evaluation board showed

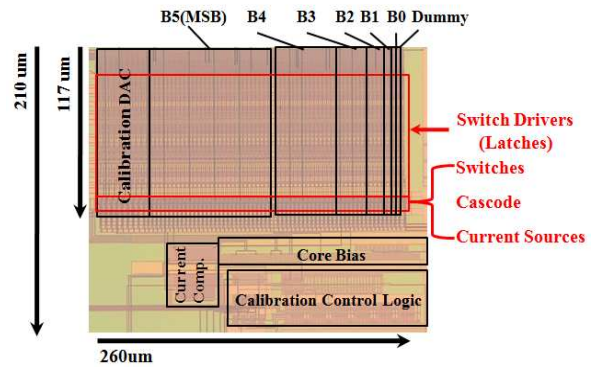


Fig. 6. Chip photo of the prototype 6-bit DAC.

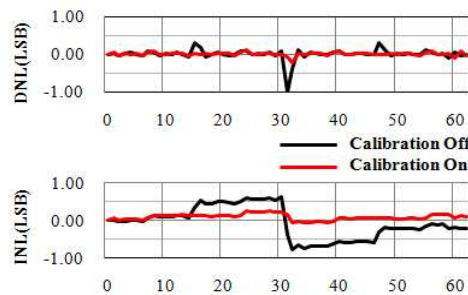
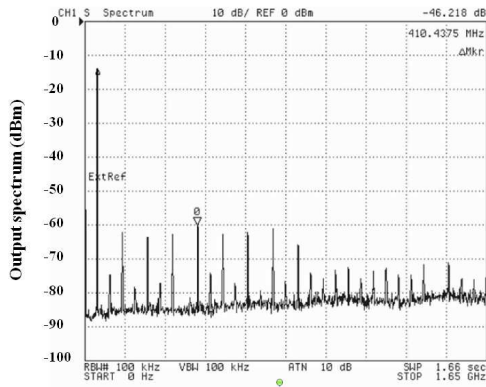


Fig. 7. Measured DNL and INL profiles.

degrading performance as the frequency increases.

Table 2 summarizes the measured performances of the proposed DAC. Performance comparison is shown in Table 3. Both [1] and the proposed design basically do not have the problem for the operation in  $3 \text{ GS/s}$



**Fig. 8.** Measured output spectrum for a 51 MHz input at 3.3 GS/s.

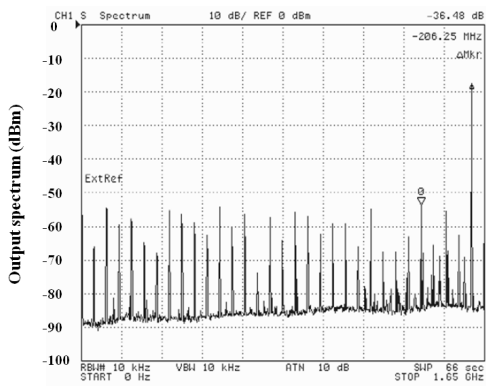


**Fig. 9.** Measured output spectrum for a 1.596 GHz input at 3.3 GS/s.

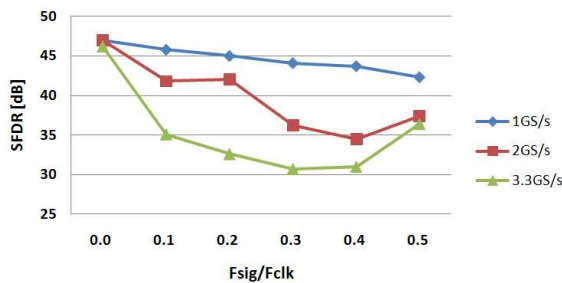


**Fig. 10.** Measured SFDR for 1 G, 2 G, and 3.3 GS/s.

sampling rate. However, in the simulation, the proposed DAC showed wideband output impedance up to 6 GS/s while conventional cascade design showed limited output impedance up to 3 GS/s. Thus, the proposed SUC is potentially suitable for future high-speed wideband application. Unfortunately, our design did not show such a good performance in the measurement due to impedance matching.

The proposed design occupies the smallest possible area, only 0.0546 mm<sup>2</sup>. Due to the complicated latch design according to [2], power consumption is larger

**Table 2.** Performance summary

Resolution		6-bit
Analog / Digital Supply		1.2 / 1 V
Conversion Rate		3.3 GS/s
Power Dissipation		47 mW
SFDR	16M, 484 MHz @ 1 GS/s	47 dB, 42.3 dB
	31M, 968 MHz @ 2 GS/s	47 dB, 37.4 dB
	51M, 1.59 GHz @ 3.3 GS/s	46.2 dB, 36.4 dB
DNL / INL		-0.22 / 0.25 LSB
Core Area		0.21 mm x 0.26 mm

**Table 3.** Performance comparison

	[1]	[10]	This work
Technology	130 nm	130 nm	90 nm
Supply Voltage	1.2 V	1.2 V	1.2 / 1 V
Resolution	6 bit	6 bit	6 bit
Conversion Rate	3 GS/s	2.7 GS/s	3.3 GS/s
Output Bandwidth	1.426 GHz	520 MHz	1.596 GHz
Segmentation	4(Una) + 2(Bin)	4(Una) + 2(Bin)	6(Bin)
Power Dissipation	29 mW	28 mW	47 mW
INL / DNL	0.02 LSB	0.1 LSB	0.25 / 0.22 LSB
SFDR	36.2 dB	37 dB	36.4 dB
Core Area	0.2 mm <sup>2</sup>	0.76 mm <sup>2</sup>	0.055 mm <sup>2</sup>
Calibration	NO	NO	YES

**Table 4.** Dynamic power dissipation

Analog	Unit current cell and bias	4 mW
Digital	Latches (63 Core, 7 Calibration)	21 mW
	Buffer, Calibration Logic	22 mW
Total Power		47 mW

than other designs. Power consumption information of a proposed design is given in Table 4.

## VI. CONCLUSIONS

This paper presented a design methodology for realizing a full binary DAC that provides good dynamic linearity at high frequency. The stacked unit cell structure minimizes the active area of the DAC and the parasitic capacitance of the current sources, which maintain high output impedance at high frequency. Although the prototype did not show constant performance for the entire range of output signal frequency, it exhibited dynamic performance at the Nyquist frequency superior to that of the state of the art 6-bit DAC. The design strategy can be useful for wideband DAC design for future communication applications.



## ACKNOWLEDGMENTS

This work was supported by the IT R&D program of MKE/KEIT [2009-S-025-01]. The CAD tools were supported by IDEC of KAIST.

## REFERENCES

- [1] X. Wu, P. Palmers, M. S. J. Steyaert, "A 130 nm CMOS 6-bit Full Nyquist 3 GS/s DAC," *IEEE J. Solid-State Circuits*, pp. 2396-2403, Nov. 2008.
- [2] A. V. d. Bosch, M. A. F. Borremans, M. S. J. Steyaert, and W. Sansen, "A 10-bit 1-GSamples Nyquist current-steering CMOS D/A converter," *IEEE J. Solid-State Circuits*, pp. 315-324, May. 2001.
- [3] J. Bastos, A. M. Marques, M. S. J. Steyaert, and W. Sansen, "A 12-bit intrinsic accuracy high-speed CMOS DAC," *IEEE J. Solid-State Circuits*, pp. 1959-1969, Dec. 1998.
- [4] G. A. M. V. D. Plas, J. Vandebussche, M. S. J. Steyaert, W. Sansen, and G. G. E. Gielen, "A 14-bit intrinsic accuracy  $Q^2$  random walk CMOS DAC," *IEEE J. Solid-State Circuits*, pp. 1708-1718, Dec. 1999.
- [5] Min-Jung Kim, Hyuen-Hee Bae, Jin-Sik Yoon, and Seung-Hoon Lee, "A 3V 12b 100MS/s CMOS D/A Converter for High-Speed Communication Systems," *Journal of Semiconductor Technology and Science*, pp. 211-216, Dec. 2003.
- [6] M. J. M. Pelgrom, A. C. J. Duinmaijer, and A. P. G. Welbers, "Matching properties of MOS transistors," *IEEE J. Solid-State Circuits*, pp. 1433-1439, Oct. 1989.
- [7] A. V. d. Bosch, M. S. J. Steyaert, and W. Sansen, "SFDR-bandwidth limitations for high speed high resolution current steering CMOS D/A converters," in *Proc. 6th IEEE Int. Conf. Electronics, Circuits and Systems*, pp. 1193-1196, Sep. 1999.
- [8] B. Razavi, *Principals of Data Conversion System Design*, New York: IEEE Press 1995.
- [9] M. Tiilikainen, "A 14-bit 1.8-V 20-mW 1-mm<sup>2</sup> CMOS DAC," *IEEE J. Solid-State Circuits*, pp. 1144-1147, July. 2001.
- [10] J. J. Jung, B. H. Park, S. S. Choi, S. I. Lim, and S. Kim, "A 6-bit 2.704Gsps DAC for DS-CDMA

UWB," *IEEE Asia Pacific Circuits and Systems*, pp. 347-350, Dec. 2006.



**Si-Nai Kim** received a B.S. degree in electrical engineering from Hongik University, Korea, in 2004, and an M.S. degree in electrical engineering from Hanyang University, Korea, in 2007. He is currently pursuing a Ph.D. degree in the Department of

Electrical Engineering at the Korea Advanced Institute of Science and Technology (KAIST), Korea. His interests include analog and mixed signal IC design.



**Wan Kim** (M'11) received a B.S. degree with highest honors in Electronic Engineering from Inha University, Incheon, Korea in 2008, and an M.S. degree in Information & Communications from Gwangju Institute of Science and Technology

(GIST), Gwangju, Korea in 2010. He is currently working toward a Ph.D degree in Electrical Engineering at the Korea Advanced Institute of Science and Technology (KAIST), Daejeon, Korea. His research interests include digital calibration techniques for high resolution data converters, and low power mixed-signal circuit design.



**Chang-Kyo Lee** (M'07) received a B.S. degree in electric engineering from Sogang University, Seoul, Korea in 2005, and an M.S. degree in information & communications from Gwangju Institute of Science and Technology, Gwangju, Korea in 2007.

He is currently working toward a Ph.D degree in information & communications at the Korea Advanced Institute of Science and Technology (KAIST), Daejeon, Korea. His research interests are in high-speed, high-resolution data converter design and low power techniques for mixed-signal circuits design.



**Seung-Tak Ryu** (M'06) received a B.S. degree in electrical engineering from Kyungpook National University, Korea, in 1997, and M.S. and Ph.D. degrees from Korea Advanced Institute of Science and Technology (KAIST) in 1999 and 2004,

respectively. From 2001 to 2002, he was with the University of California at San Diego as a visiting researcher, sponsored through the Brain Korea 21 (BK21) program. In 2004, he joined Samsung Electronics in Kiheung, Korea, where he was involved in mixed-signal IP design. From 2007 to 2009, he was with the Information and Communications University (ICU), Daejeon, Korea, as an Assistant Professor. Since 2009, he has been with Korea Advanced Institute of Science and Technology (KAIST), Daejeon, Korea, in the Department of Electrical Engineering as an Assistant Professor. His research interests include analog and mixed signal IC design with an emphasis on data converters.